Soil pore system complexity and heterogeneity as affected by contrasting management practices

Jocenei A. T. de Oliveira[1], Luiz F. Pires[2], Fabio A. M. Cássaro[2], José V. Gaspareto[1], Adolfo N. D. Posadas[3], Sacha J. Mooney[4],

[1] Physics Graduate Program, State University of Ponta Grossa, 84.030-900 Ponta Grossa, PR, Brazil

[2] Laboratory of Physics Applied to Soil and Environmental Sciences, State University of Ponta Grossa, 84.030-900 Ponta Grossa, PR, Brazil

[3] AgriEntech Ltda., São Carlos-SP, Brazil

[4] Division of Agricultural and Environmental Sciences, School of Biosciences, University of Nottingham, Sutton Bonington Campus, Leicestershire LE12 5RD, UK

ABSTRACT

To better understand the changes that occur in soil systems at different scales, researchers have been using concepts from the multifractal theory for investigating intricate and heterogeneous complex structures. This analysis has also been applied to understand how complex systems such as the soil behave under contrasting management practices. This study presents the use of three-dimensional multifractal theory, lacunarity, and normalized Shannon entropy to characterize changes in the porous system of a Rhodic Hapludox under different management practices (conventional tillage, minimum tillage, and no-tillage) compared with the same soil under a secondary forest, as a reference. The results of lacunarity and multifractal spectra revealed separations between management groups in relation to their porous systems (secondary forest with no-tillage and conventional tillage with minimum tillage). These results indicate possible "degradation" in the structure of the soil under conventional and minimum tillage and its preservation when under no-tillage as the complexity of their pores is analyzed. The contrasting management practices and forest presented linear correlations between soil porosity and lacunarities, maximum normalized Shannon entropy, and the multifractal spectra. The degree of multifractal spectra asymmetries and lacunarities evidenced the variability of

spatial distributions of the managements and forest pore size diameters, showing that these tools are useful for characterizing the soil pore system. The results obtained showed the potential and sensitivity of the 3D multifractal approach in the characterization and differentiation of complexity in soil management practices.

Keywords: Fractal dimension, lacunarity, X-ray microtomography, 3D image analysis, soil structure, management practices.

1. Introduction

In recent decades, fractal and multifractal theory has been applied in studies that intend to improve the knowledge of natural and artificial processes, from the macroscopic to the microscopic points of view. The use of this approach can provide details concerning non-linearity and high complexity of porous systems (Pachepsky et al., 2006; Pachepsky et al., 2000; Brown et al., 2002; Mandelbrot, 1983). Thus, the random behavior, often exhibited by numerous phenomena that occur in nature, makes their analysis, in most cases, an extremely complex task. It means that non-conventional methodologies of analysis can be useful for evaluating the structure of complex systems.

In many investigations the fractal theory has been able to provide a better understanding and interpretation of complex, dynamic, and non-linear systems through the analysis of self-similar and non-Euclidean patterns (Monreal et al., 2013; Mandelbrot, 1983). Distribution of probabilities, related to the multifractal theory, can be used for studying physical and thermodynamic properties of complex three-phase systems such as soils (Monreal et al., 2013; Chhabra et al., 1989; Chhabra and Jensen, 1989).

Fractals or multifractals are self-similar or self-affine objects which are associated with non-integer or fractional dimensions. In soil science, the multifractal

approach has been used to deal with different investigations, varying from studies to understand irregular soil particle shapes and their free scale hierarchy to the analysis of the macropore structures and preferential solute flow pathways (Luo and Lin, 2009; Posadas, 2007; Pachepsky et al., 2006, Pachepsky et al., 2000).

Parameters such as lacunarity, related to the accounting of gaps or space distributions as a staggered function, and entropy, related with the uncertainty of a given physical measurement, have been employed in the study of different phenomena (Roy and Perfect, 2014; Gould et al., 2011; Posadas et al., 2005, Posadas et al., 2003; Chun et al., 2008; Chhabra et al., 1989; Chhabra and Jensen, 1989; Mandelbrot, 1983). These parameters together with multifractal analysis can be used to characterize the heterogeneity and complexity of porous systems, such as soils. It is important to emphasize that many times, just the evaluation of morphological and geometric properties of the soil cannot provide information about the complexity of its pore system.

Advances in X-ray Computed Tomography (XCT) combined with the development of digital image processing have been permitting more detailed studies of the architecture of the soil pore system (de Oliveira et al., 2021; Li et al., 2019; Wang et al., 2017). Using three-dimensional (3D) analysis of soil images at the micrometer scale, soil scientists have been achieving a better understanding of many processes and phenomena that occur in this porous medium (e.g. water retention and conduction, gas transport, chemical elements migration, etc.) (Borges et al., 2019; Galdos et al., 2019; Ferreira et al., 2019; Munoz-Ortega et al., 2015; Dal Ferro et al., 2012). Moreover, geometric parameters such as pore connectivity (C) and tortuosity (τ), as well as the heterogeneity of the porous medium, expressed by the degree of anisotropy (DA), can also be measured when 3D analyses are performed (Borges et al., 2019; Pires et al., 2019a,b; Torre et al., 2018; Martínez et al., 2017; Sampurno et al., 2016; Roque et al.,

2012; Martínez et al., 2010). These parameters can be employed for a better comprehension of the processes that take place inside the soils.

The vast majority of the recent research using the multifractal theory as an investigation tool is based on the analysis of two-dimensional (2D) images. Since soil porous systems are three-dimensional it is reasonable to extend this investigation for 3D images. This is made applying multifractal concepts such as lacunarity and entropy for investigating 3D images obtained by XCT (Soto-Gómez et al., 2020; Torre et al., 2018; Sampurno et al., 2016; Martínez et al., 2010).

Despite several papers dealing with XCT to analyze properties of soil pore systems based on their morphological and geometrical properties (Camargo et al., 2022; Bhattacharyya et al., 2021; Martinez-Carvajal et al., 2019; Zhu et al., 2016), the use of characterization parameters that evaluate the complexity and heterogeneities of the architecture of the pores has not been extensively applied; mainly in the evaluation of the effect of management practices in the soil structure of tropical soils. Differences observed in the porous system of tropical soils in comparison to those under temperate climate conditions, make crucial the characterization of their structures. This is mainly important as tropical soils are frequently exposed to heavy precipitation events, which require soils with adequate infiltration capacity.

The approach used in this paper was to apply 3D multifractal theory concepts such as: lacunarity analysis, multifractal spectrum, entropy examination, and degree of multifractality (Δ) aiming the characterization and evaluation of changes in the porous system of an Oxisol under three contrasting management practices. Also, geometric parameters (C and τ) and pore system heterogeneity analysis (DA) were used for complementing the characterization of the soil pore space. From this conceptualization, a detailed analysis of the soil structure complexity was provided and a better

discrimination of the effect of management practices on the soil structure could be revealed.

2. Material and methods

2.1. Collection of the samples

The soil samples were collected at the experimental farm of the Agronomic Institute of Parana located in the city of Ponta Grossa, State of Paraná, Brazil (25°09' S, 50°09' W, 875 m a.s.l). According to the classification presented by the Soil Survey Staff (2013), the soil is characterized as a Rhodic Hapludox (Oxisol). The investigated soil samples are from plots where three contrasting management practices are conducted (conventional tillage – CT, minimum tillage – MT, and no-tillage – NT). An area under secondary forest (F) was used as a reference. We will also consider the samples under F as management throughout this paper. A total of 20 samples were collected for this study (5 samples for each management practice + 5 samples for F).

The soil had the following average composition in terms of constituents: 578±34 g kg^{-1} of clay, 280±52 g kg^{-1} of silt, and 142±49 g kg^{-1} of sand and was classified as clayey according to the USDA textural classification triangle (Hillel, 2003). The experimental plots studied here have areas of c. 1.0 ha (NT) and c. 0.6 ha (CT and MT), respectively. The tillage systems had been employed in the areas for over 35 years at the time of the sampling. The experimental areas of CT, MT, and NT were initiated in 1981 after the conversion of part of secondary forest to pasture-land (Sá et al., 2015). Under CT, the soil was submitted to discing at 25 cm depth followed by 10 cm harrowing twice a year after summer and winter harvesting procedures. The soil under MT, was prepared using a chisel cultivator at 25 cm depth followed by a 10 cm narrow disking, causing minimum

soil disturbance, and the crop residues were maintained at the soil surface. The area under NT was not submitted to any soil preparation (just planting procedures).

In the experimental sites, crop rotation was performed, with cover crops [oats (*Avena strigosa*) or vetch (*Vicia sativa*)] or wheat (*Triticum aestivum L.*) in winter and corn (*Zea mays*) or soybean (*Glycine max*) in summer. The operations of soil and crop management, sowing and harvest, were made with commercial tillage machines (e.g. tractors). The traffic in the NT area was restricted to sowing equipment with a cutting disc for sowing the summer and winter crops. Each experimental area (NT, CT, and MT) was submitted to 8-9 soil interventions through the year (clearing, planting seed, and soil preparation operations) using tractors (MF 275F), weight around four tons .

Soil sampling was carried out at the beginning of 2017 at the surface layer (0-10 cm) after corn harvest at the crop rows, to avoid possible effects of tractor wheel traffic (clean, plant seed, and soil preparation operations) on soil structure. For CT, sampling occurred almost six months after plowing and harrowing operations, which allowed the collection of soil samples at natural reconsolidated stages. NT, MT, and F samples were collected at the same sampling time of CT. Core samples were performed using stell cylinders 5.0 cm high and 4.8 cm inner diameter (around 91 cm^3) attached to a core sampler. Sampling was undertaken very carefully, in order not to introduce soil compaction during extraction and handling. Since the soil water content is very important at sampling time, to minimize damage in the soil structure, samples were collected near their field capacity, which occurred about three days after a high-intensity rainfall event. After sampling, the samples were wrapped in plastic bags and transported to the laboratory. The soil excess outside the steel cylinders was carefully trimmed off, using a sharp knife, and the top and bottom surfaces of the sample were flattened, which make the sample volume equal to the internal volume of the cylinder.

2.2. Image Acquisition and Processing

After the previous preparation, the samples were sealed with a very thin layer of paraffin and transported to The Hounsfield Facility, University of Nottingham (Sutton Bonington Campus). There they were scanned using a GE XCT scanner, model v | tomex | m, operating with a voltage of 180 kV, current of 160 µA, and acquisition time of each image of 250 ms. To minimize beam-hardening effects a 0.1 mm Cu-filter was placed between the source and the sample and detector. A total of 20 samples (management practices + secondary forest – 5 of each) were scanned for 3D XCT analysis. The images were reconstructed in 32 bits, avoiding overlapping gray tones. To minimize possible artifacts due to border effects from the sample collection, the volume of interest (VOI) was selected between 7 and 10 mm away from the sample edges (Pires et al., 2004).

A total of 2,520 projections were obtained per sample. The 3D final image consisted of a stack of 860 2D images (860 by 860 pixels), acquired along the longitudinal direction (z) of the samples. After reconstruction, the images were imported into Volumetric Graphics (VG) StudioMAX® 2.0 and cropped to a cubic shape, with 30.1×30.1×30.1 mm^3 (860×860×860 voxels) and a voxel size of 35 µm. For the segmentation and binarization of the images, the non-parameterized Otsu method (horizontal layer-wise) from ImageJ 1.42 software was used. In this stage, the raw images (in shades of gray) were processed using a 3D Median filter (noise reduction) and unsharp mask (standard deviation 1 voxel and weight 0.8) to enhance the borders. The remove outlier tool, with a radius of 0.75, was applied in the images after segmentation. At the end of these steps, a set of binary images (zeros and ones) was obtained, in which white represented the pores and black represented the soil matrix.

2.3. 3D Lacunarity, Multifractal analysis, and Normalized Shannon Entropy

For the calculation and determination of 3D lacunarities (Λ) (for better interpretation, see the supplementary material for more details about 3D lacunarity analysis) , a script was written in the Matlab® environment using the box-counting method with the application of Eq. 1. Cubic box sizes (ε) related to the 860 divisors (12 divisors – 1, 2, 4, 5, 10, 20, 43, 86, 172, 215, 430, and 860) were selected to start the calculation from the major to the minor box by time optimization (Dong, 2000; Sarkar and Chaudhuri, 1995). Lacunarity (Eq. 1) is dependent on the size of the box (scale), that is, as a rule, the larger the size of the box, the smaller the value of the lacunarity (Martínez et al., 2017):

$$\Lambda(\varepsilon) = \frac{\sum_s s^2 P(s,\varepsilon)}{[\sum_s sP(s,\varepsilon)]^2} = \frac{Z(2)}{[Z(1)]^2} \qquad (1)$$

where s is the number of black pixels, ε is the box size, P (s,ε) are the distribution probabilities, Z(1) and Z(2) are associated with the first and second moments of the distribution.

The lacunarity can also be expressed in terms of mean values ($\bar{\mu}$) and variances (σ) of the box probability density distributions:

$$Z(1) = \bar{\mu} \text{ and } Z(2) = \bar{\mu}^2 + \sigma^2 \qquad (2)$$

$$\Lambda(\varepsilon) = \frac{Z(2)}{[Z(1)]^2} = \frac{\sigma^2}{\bar{\mu}^2} + 1 \qquad (3)$$

For a better analysis of the linear behavior trend of the lacunarity curves, they were divided into three parts with the following intervals: 1–10 voxels (first part), 20–172 voxels (second part), and 215–860 voxels (third part). After calculating the linear adjustments in each of these parts, the linear behaviors were confirmed by the analysis of the determination coefficients (r^2) larger than 0.90.

The first-order derivative of the lacunarity curves, which permits the analysis of maximum and minimum inflection points, was obtained using the methodology presented by Roy et al. (2014):

$$\frac{\mathrm{d}\ln\Lambda(\varepsilon)}{\mathrm{d}\ln\varepsilon} = \frac{\ln\Lambda(\varepsilon_{i+1}) - \ln\Lambda(\varepsilon_{i-1})}{\ln\varepsilon_{i+1} - \ln\varepsilon_{i-1}} \quad (4)$$

where i is an index that is related to each point on the curve.

In this paper, the multifractal parameters α_{max} and $f(\alpha_{max})$, which represent the internal energy and the entropy (like Boltzmann entropy) of the system (Chhabra et al., 1989), were used to characterize the analyzed soil systems. Both parameters were obtained from the 3D multifractal spectra curves.

For the analysis, interpretation, and quantification of 3D multifractal spectrum curves (see the supplementary material for more details regarding the 3D multifractal analysis), parameters such as the degree of multifractality (Δ) and the asymmetry (A) of the spectrum were calculated (Szczepaniak and Macek, 2008):

$$\Delta = \alpha_{maximum} - \alpha_{minimum} \quad (5)$$

$$A = \frac{\alpha_0 - \alpha_{minimum}}{\alpha_{maximum} - \alpha_0} \quad (6)$$

where $\alpha_{maximum}$ and $\alpha_{minimum}$ are Lipschitz–Hölder exponent maximum and minimum of the multifractal spectrum and α_0 is the value of the Lipschitz–Hölder exponent at q=0.

It is known that high numerical values of the degree of multifractality are associated with greater heterogeneities of the porous medium. Positive values of the asymmetry (A>1) indicate asymmetry to the left side of the spectrum (higher pore amounts); while positive (A<1) indicate asymmetry to the right side of the multifractal curve (region of the solid part of the structure); and, finally, when the asymmetry is equal to the unit (A=1), the spectrum is symmetrical for both sides (pores and solids).

3D normalized Shannon entropy (Eq. 7) (for better interpretation, see the

supplementary information for more details about 3D normalized Shannon entropy analysis) was used for detecting distinctions in the porous system heterogeneity (Chun et al., 2011, 2008):

$$H^*(\varepsilon) = \frac{H(\varepsilon)}{H_M(\varepsilon)} = -\frac{1}{\log(\varepsilon^3+1)}\sum_{i=0}^{\varepsilon^3} P_i(\varepsilon)\log P_i(\varepsilon) \quad (7)$$

The 3D multifractal spectrum was determined using box sizes of 5, 10, 20, 43, 86, 172, 215, and 430, and distribution moments (q's) ranging from -1.4 to 2.0 with regular steps of 0.1. Better refinements of standard entropies were obtained using box sizes of 30, 35, 40, 45, 50, 60, 65, 70, 75, 80, 90, and 100. For the quantification of the multifractal spectra and normalized Shannon entropies, the NASS (*Non-linear Analysis Scaling System - AgriEntech Ltda/Rutgers University*) software was used. The software is based on the canonical method introduced by Chhabra et al. (1989), Posadas et al. (2005), and Chun et al. (2008).

2.4. 3D Geometric Parameters

The pore connectivity (C) was measured using the BoneJ plugin from ImageJ-Fiji (1.52) software. The images were firstly filtered utilizing the *purify* filter (*connectivity* function) (Dal Ferro et al., 2014; Doube et al., 2010) and then the pore connectivity was obtained employing the following equations:

$$C = 1 - EN \quad (8)$$

$$EN = n_v - C_v \quad (9)$$

where EN is the Euler number, n_v is the number of disconnected parts of the porous space per volume, and C_v is the connectivity by volume. For better analysis and interpretation of C, we renormalized their values (a division of C by the 3D reconstructed volume).

Tortuosity (τ), defined by the ratio of the geodesic distance (L_G), between two points connected in the pore network, and the Euclidean distance (L_E) between them, was

calculated using equation 10, implemented in the *OsteoImage* software developed by Roque et al. (2009, 2012) (Borges et al., 2019; Pires et al., 2019a,b; Roque et al., 2012, 2009):

$$\tau = \frac{L_G}{L_E} \qquad (10)$$

The degree of anisotropy (DA), which is a measure of how the substructures are arranged, aligned, and oriented within a region of interest, was calculated employing the mean intercept length method implemented in the BoneJ plugin (Tseng et al., 2018; Doube et al., 2010):

$$DA = 1 - \frac{\text{Eigenvalue}_{\text{minimum}}}{\text{Eigenvalue}_{\text{maximum}}} \qquad (11)$$

where the eigenvalues minimum and maximum refer to the minimum and maximum radii of the structure of an ellipsoid. The degree of anisotropy values varies from 0 (completely isotropic pore system medium) to 1 (completely anisotropic pore system medium).

2.5. Statistical Analysis

Before any statistical analysis, all data were tested to verify their normality and homoscedasticity. Analysis of variance (ANOVA) and Tukey HSD test (p<0.05) were applied to the results of f(α_{max}), α_{max}, Δ, A, C, τ, and DA. The PAST (PAleontological STatistics) program version 3.21 was used in our statistical analyses (Hammer et al., 2001).

3. Results and Discussion

3.1. 3D Lacunarity (Λ)

The results of the 3D lacunarity sectioned graphs (first, second, and third parts) show that F and NT had the highest values of lacunarity when compared to MT and CT

(Fig. 1a). The existence of bio pores and fissures usually present in soils under F and NT can explain the highest values of lacunarity found for these two managements (Luo and Lin, 2009; Tavares et al., 2009). The higher amounts of organic material (not evaluated in our study) generally found in conservationist systems, such as NT and F, are associated with the active action of the soil fauna, contributing to the formation of biopores. In addition, the presence of these types of pores contributes to the diversity and complexity of the pore system (Bhattacharyya et al., 2021; Galdos et al., 2019; Borges et al., 2019). Recently, Pires et al. (2019a) published a study with the same soil and management practices as those discussed here. More detailed information related to the influence of organic matter on soil porosity and other soil properties is better discussed there. In addition, they verified the relation between the organic carbon amount and the structure of an Oxisol. The results of these authors agree with those demonstrated in our study concerning the architecture of the pores.

According to Martínez et al. (2017) and Tseng et al. (2018), lacunarity and porosity are quantities inversely related when the distributions of occupied spaces inside each cubic box are analyzed. It means that as the fraction occupied by lacunes or spatially empty spaces increases, higher is the lacunarity and lower is the porosity; in other words, the greater the fraction occupied by "distributions of lacunes" or spatially empty spaces, the greater will be the lacunarity and smaller will be the porosity. Thus, the imaged porosity obtained for F and NT (14% and 11%) is an indication of the high lacunarity value found for these two managements. On the opposite, the small lacunarity values found for MT and CT is related to the largest imaged porosities of 21% and 24% for these managements (Fig. 1c).

Porosity results presented in Pires et al. (2019a), which investigated the same soil and management practices, consubstantiate the lacunarity results here obtained. It

was also found the presence of pores with different shapes (not covered in this paper) on the soil matrix of all managements, which certainly influenced the lacunarity behavior here found. The lacunarity is also related to the variability of the spatial distribution of pore size patterns, while the porosity expresses only the volume of pores in the samples (Santos et al., 2020; Tseng et al., 2018). This fact highlights the importance of the use of lacunarity to characterize the soil pore system.

The lacunarity curves were sectioned in parts where a linear behavior 0.00 - 2.30, 3.00 - 5.15, and 5.37 - 6.76 was observed. These sections were named as first, second, and third sections (see Fig. 1a). A decreasing behavior was observed according to the scale of analysis, as already verified in the papers by Luo and Lin (2009), Monreal et al. (2013), and Martínez et al. (2017). The linear regressions (Fig. 1a) showed correlation coefficients around 0.98 (first and second parts) and 0.96 (third part); which is an indication of the existence of high linearity and self-similarity of dispersion patterns and pore clusters in the porous spaces studied (Martínez et al., 2017; Monreal et al., 2013; Luo and Lin, 2009). It is worth mentioning that the existence of pore clusters has a significant influence on the transport, conduction, redistribution, and deposition of fluids (water and gases) in the soil, which are essential for plant growth and development (Camargo et al., 2022; de Oliveira et al., 2021; Galdos et al., 2020, 2019; Borges et al., 2019; Dal Ferro et al., 2014).

The high similarity of the 3D lacunarity curves (Fig. 1a) allowed us to separate the samples into two groups (F with NT and CT with MT). This result is even more evident when the minimum inflection points of the derivative curves are analyzed (Fig. 1b). It was noticed that the inflection points of CT an MT were very close to each other, and they occurred for smaller cubic box sizes, around 10 voxels (0.35^3 mm^3 – first part) (ln10 = 2.30). For F and NT, the inflection points occurred in cubic box sizes 4 times

larger, around 43 voxels (1.50^3 mm^3 – second part) (ln43 = 3.76). The two groups (F and NT and CT and MT) also exhibited differences in the derivative curves in the transitions from the first to the second part, where there is an abrupt drop for a given box size range (1 to 5 voxels and 5 to 43 voxels). On the other hand, for the second size range, from 5 to 43 voxels, there is a small plateau or constant region of the curve for CT and MT (Fig. 1b), which is associated with lower patterns of spatial distributions of the pore space when compared to other groups mentioned earlier (Roy et al., 2014; Monreal et al., 2013; Luo and Lin, 2009).

3.2 3D Multifractal spectra, multifractal parameters, and normalized Shannon entropy

The analysis of the multifractal spectra (Fig. 2) also showed similarities between groups of management practices (F with NT and CT with MT). The same tendency as observed for lacunarity results was also noticed. The multifractal spectra obtained are asymmetrical, especially for F and NT, whose results are corroborated by the values of the degree of asymmetry (Table 1). Similar results, referring to the shapes of the multifractal spectra, were found in Martínez et al. (2010) and Torre et al. (2018). These authors also analyzed soils submitted to different management practices.

High values related to the degree of multifractality in Table 1 reflect the heterogeneity and complexity of the porous system studied (Torre et al., 2018; Wang et al., 2018; Martínez et al., 2010; Posadas et al., 2003). As it can be seen, there were no significant differences among managements and forest for the degree of multifractality. According to Martínez et al. (2010), Siqueira et al. (2013), and Leiva et al. (2019), asymmetries of the multifractal curves to the right side (Fig. 2), show the prevalence of higher singularity points (α), indicating lower concentrations of measures and values of $q<0$ (lower spatial variability of pore concentrations). In Posadas et al. (2005), similar

spectra results (degree of asymmetry for the right side) were related to low patterns of spatial variability of the ulexite mineral. In our paper, this asymmetry is related to the low spatial variability of large or thick pores, as shown in Fig. 3.

Thus, the lower values of the degree of asymmetry (Table 1) for CT and MT indicate low variability of spatial distributions of large pore clusters (Figs. 3b,c) over the investigated sample volumes. These large pore clusters (diameters of 100 to 500 μm) were concentrated in certain spatial regions of the studied sample volumes. This suggests the presence of isolated pores (not connected to the rest of the pore network but locally connected). In the 3D images presented in Fig. 3 are possible to observe the existence of some clusters of isolated pores for CT and MT, corroborating the results obtained for the asymmetry. For F and NT (Table 1), the higher degree of asymmetry indicates a more homogeneous distribution of pore clusters within the sample volumes (Figs. 3a,d). Such result implies a better continuity of the pores across the entire sample volumes, indicating more appropriate soil structures for agriculture practices, water movement and water retention, root development, etc (de Oliveira et al., 2021; Pires et al., 2019a; Blanco-Canqui et al., 2017; Tavares et al., 2009). An analysis of the 3D images for F and NT (Figs. 3a,d), at least for the pores visualized at the higher portion of the images, allowed us to observe the presence of several pores connected through channels for these two managements, which are essential in water transport properties.

The multifractal parameters α_{max} and $f(\alpha_{max})$ exhibited the same tendency of separation for the other parameters analyzed (F with NT and CT with MT) (Table 1). Physically, α_{max} and $f(\alpha_{max})$ are associated with the internal energy and Boltzmann's entropy (or average global entropy) of the systems analyzed. The internal energies and global entropies were higher for CT and MT when compared to F and NT (Table 1). The internal energy is related to the configurational states of a system. Abrupt changes in its

value are related to internal energy increasings. Thus, samples under CT and MT were characterized by more significant variations in their internal energies, and more entropy, which is an indication of the vulnerability of their porous systems to changes, mainly in CT. Management practices such as those of CT and MT are subjected to the inversion of the superficial layers of the soil by mixing different soil layers, which promotes disorganization of their pore networks, resulting in higher values of the entropy associated with the pore system (Blanco-Canqui et al., 2017; Imhoff et al., 2010; Posadas et al., 2009; Posadas, 2007).

Soils submitted to lower soil preparation practices, e.g., no-tillage, are expected to present low entropies and internal energy values as illustrated in our study. In a study involving water retention curves and pore functionality on the same soil, de Oliveira et al. (2021) showed that CT and MT had a higher percentage of fissure pores concerning to transmission pores through 3D image analysis. Fissure pores represent the breakdown of the porous structure. It produces the increase of energy dissipation and entropy (Addiscott, 1995). Such result support the disorganization of the pore space of the mentioned managements, their high values of internal energy, global entropy, and maximum normalized 3D Shannon entropy.

Analyzing the normalized 3D Shannon entropy (Fig. 4a), the peaks show that F and NT had the lowest $H^*(\varepsilon)_{max}$ (0.81 and 0.79) when compared to CT and MT (0.88 and 0.86). These results corroborate those quantified through 3D multifractal spectra ($f(\alpha_{max})$– Boltzmann's entropy) and, in fact, demonstrate the greater heterogeneity and disorganization of the pore space of the last two mentioned management practices. For F, CT, and MT, the values of $H^*(\varepsilon)_{max}$ occurred for cubic boxes of 20 voxels (optimal values), while for NT, 30 voxels. According to Chun et al. (2008), entropy is a measure of the randomness or uncertainty within a set of elements, which in the case of soil

samples is represented by differences in the abundance of pores or solid particles within their volumes.

Lower pore occupancy rates and, therefore, lower values of $H^*(\varepsilon)_{max}$ were observed as the cubic sizes increased for NT; the opposite behavior was verified for CT. It is an indication that in no-tillage, the probability $P_i(\varepsilon)$ of finding pores decreased as the investigated volume increased; that is, there is a smaller amount of pores or clusters of pores of certain sizes in diameter (Chun et al., 2008). The maximum entropy is obtained when all possible values of i, the number of pixels or voxels corresponding to the pores in a cube with a volume ε^3, are equiprobable; that is, they have the same probability $P_i(\varepsilon)$ of occurrence. Thus, the normalized Shannon entropy provided the degree of information or uncertainty of the pore occupation rate (number of pores with a certain diameter) as a function of the scale (Fig. 4a). It also permitted separating the contrasting managements into two distinct groups, as previously mentioned.

From another point of view, the complexity of the pore size distribution increased as the size of the investigation box decreased, as the rate or probability of occupying this box by pores became higher (Wang et al., 2008; Posadas et al., 2003). In this perspective, higher values of maximum normalized Shannon entropy for CT and MT revealed a greater richness in the range of pore sizes, implying a great heterogeneity (complexity) of the porous system in these treatments. The opposite was verified for F and NT (Fig. 4a), which is an indication of more homogeneous pore systems for these managements as compared to CT and MT. The concentration of pore clusters and the presence of isolated pores for the last ones can help explain the results found for maximum normalized Shannon entropy.

Finally, the linear relationships between the maximum normalized Shannon entropy ($H^*(\varepsilon)_{max}$) and the Boltzmann's entropy ($f(\alpha_{max})$) related to the porosities are

presented in Figs. 4b,c. Finally, by using multifractal tools to characterize these porous media, it was noticed that samples soils under CT and MT exhibited the more heterogeneous porous systems as compared to the other ones.

3.3 3D Geometric Parameters

The degree of anisotropy (DA) did not exhibit significant differences among managements, which is indicative that they did not affect the soil structure as compared to F (Table 2). Degree of anisotropy values close to 0 mean isotropic porous systems. The results observed here are supported by Dal Ferro et al. (2014) and Pires et al. (2019a,b), who investigated the same soil type and management practices. The low degree of anisotropy values (Table 2) show that the pores in the studied Oxisol do not have privileged directions. Therefore, there is a great correspondence between the different spatial orientations (x, y, z) analyzed. Another interpretation is that this parameter was not sensitive enough to demonstrate differences between porous systems in relation to pore clusters. This reinforces the use of the 3D lacunarity and multifractal analysis to characterize complex porous materials.

Regarding pore connectivity (C), significant differences were found among managements (Table 2). The value associated with the connectivity followed the sequence: CT > MT > F > NT, similar to the findings reported in Pires et al. (2019a,b). We observed that the soil usage allowed separating the soil samples again into two groups (CT and MT and F and NT). Even with the soil samples under CT and MT (Figs. 3b,c) having clusters of isolated small pores, the large ones seemed to be very connected, contributing to large values of pore connectivity found for these two managements (Camargo et al., 2022; Peth et al., 2008).

As a rule, soils under more intensive management practices are normally more susceptible to degradation, especially in tropical regions, where the structure of these soils is constituted of large amounts of non-continuous pores (Tseng et al., 2018). In this study, greater connectivity in CT may also be related to the period in which the samples were collected in the experimental field, almost six months after the plowing and harrowing operations, which permitted the soil structure from this management to reconsolidate. This means that in this period, between the intervention and the collection of samples, mainly due to the action of natural processes such as rain, soil fauna, and the root system of the cultivated crop (corn), the soil regained its pore structure and pore connectivity (de Oliveira et al., 2021; Pires et al., 2019a,b).

Lower values of connectivity observed for F and NT are not expected as these managements are more exposed to biological activities. No-tillage samples had similar pore connectivity values as compared to F. It indicates that it was the management that preserved the structure conditions more similar to F. Galdos et al. (2019) reported opposite results to those found by us for pore connectivity, which indicates that there is no consensus about this soil's physical property and management practices. Factors such as the time the management system was established, the kind of crop, the type of soil, tillage procedures, and rainfall regimes can cause the differences observed among diverse studies.

In the research by Borges et al. (2019), conducted in the same soil and experimental site studied here it was found higher saturated hydraulic conductivity for CT in comparison to NT. In principle, this is indicative of a higher pore connectivity for CT when these two management practices are compared. Despite the observed differences, the soil matrices of all the managements were characterized by highly connected pore structures, as can be seen in Fig. 3.

Regarding the tortuosity, significant differences were observed between some of the managements (Table 2). Conventional and minimum tillage samples had the lowest tortuosities, which would be expected due to the initial disruption of the soil structure caused by CT soil preparation, followed by the creation of large pore clusters produced in the soil reconsolidation (Figs. 3b,c). For NT, larger tortuosity values are mainly associated with the absence of soil structure disturbance procedures and the action of soil fauna and cover plant residues and roots, which produced a more complex pore structures (Figs. 3a,d). Pore tortuosity is an important parameter that impacts root growth, movement, and transport of mass and energy (water and gases) in the soil. Thus, it is crucial to characterize this property to infer its impact on water retention and movement (Camargo et al., 2022; Galdos et al., 2020, 2019; Borges et al., 2019).

Based on the 3D multifractal, lacunarities, entropies, and geometric parameter analyses, we noticed that NT samples presented a porous system similar to that of F. Our results indicate that even after more than 35 years under NT, the soil studied maintains an appropriate structure for both infiltration and retention of water (Borges et al., 2019; Galdos et al., 2019). In contrast, MT closely resembles CT in the complexity of the porous architecture. This finding indicates that the Oxisol under long-term MT did not have conditions to recover its structure in a similar way to F and NT managements. It is probably associated with the agriculture operations carried out in the experimental field from one crop to another (Cherubin et al., 2017; Panachuki et al., 2015). We have to mention that further studies considering different crops, size and amount of samples, pore sizes, and soil types should be proposed for a better comprehension of the effect of management practices in tropical soils under long-term experiments.

4. Conclusions

Our study highlights the importance of a 3D multifractal and lacunarity calculations to verify differences in the complexity of the soil pore system of samples under contrasting management practices (no-tillage, minimum tillage, conventional tillage, and secondary forest). Our results, mainly those of the 3D multifractal investigation, allowed the separation of the soil managements into two groups as a function of the self-similarity of their porous structures. We found that the lacunarities, entropies, and geometric parameters measured of the porous system under no-tillage is similar to that of the secondary forest. These results suggest that even after long periods under this management, the soil maintain the quality of its structure in terms of agricultural productivity.

We noticed that the 3D multifractal approach was helpful for a detailed analysis of the soil pore system under contrasting managements. Contrary to morphological and geometrical properties, the technique showed to be sensitive to detecting changes in the complexity of the pore architectures (e.g., degree of anisotropy) of the investigated soil samples. Another relevant and innovative contribution presented in our study was the proposal of the use of thermodynamic properties such as internal energy, global entropy (Boltzmann's entropy), and normalized 3D Shannon entropy with the purpose of better understand the changes caused by the management practices in the soil pore system. Until now, few studies exploring these thermodynamic properties in the field of soil science were presented. Then, we believe our results represent a vital contribution to understanding the complexity of 3D porous structures.

Acknowledgments

LFP would like to acknowledge the Brazilian National Council for Scientific and Technological Development (CNPq) [Grants 304925/2019-5 and 404058/2021-3] and the

Coordination for the Improvement of Higher Education Personnel (Capes) [Grant 88881.119578/2016-01]. JATO would like to acknowledge Capes for the Ph.D. grant (Code 001). We would like to express our gratitude to Dr. Brian Atkinson and Craig Sturrock for their expertise in X-ray Computed Tomography. Finally, we also would like to thank André L.F. Lourenço for the support in the computational and image analysis processing.

4. References

Addiscott, T.M., 1995. Entropy and sustainability. European Journal of Soil Science, v. 46, n. 2, p. 161-168. https://doi.org/ 10.1111/j.1365-2389.1995.tb01823.x

Bhattacharyya, R., Rabbi, S.M.F., Zhang, Y., Young, I.M., Jones, A.R., Dennis, P.G., Menzies, N.W., Kopittke, P.M., Dalal, R.C., 2021. Soil organic carbon is significantly associated with the pore geometry, microbial diversity and enzyme activity of the macro-aggregates under different land uses. Science of the Total Environment. 778, 146286. https://doi.org/10.1016/j.scitotenv.2021.146286

Blanco-Canqui, H., Wienhold, B.J., Jin, V.L., Schmer, M.R., Kibet, L.C., 2017. Long-term tillage impact on soil hydraulic properties. Soil Tillage Res. 170, 38–42. https://doi.org/10.1016/j.still.2017.03.001

Borges, J.A., Pires, L.F., Cássaro, F.A., Auler, A.C., Rosa, J.A., Heck, R.J., Roque, W.L., 2019. X-ray computed tomography for assessing the effect of tillage systems on topsoil morphological attributes. Soil Tillage Res. 189, 25-35. https://doi.org/10.1016/j.still.2018.12.019

Brown, J.H., Gupta, V.K., Li, B.L., Milne, B.T., Restrepo, C., West, G.B., 2002. The fractal nature of nature: power laws, ecological complexity and biodiversity. Philos

Trans R Soc Lond B Biol Sci. 357 (1421), 619-626. https://doi.org/10.1098/rstb.2001.0993

Camargo, M.A., Cássaro, F.A.M., Pires, L.F., 2022. How do geometric factors influence soil water retention? A study using computerized microtomography. Bull. Eng. Geol. Environ. 81, 137. https://doi.org/10.1007/s10064-022-02632-z

Cherubin, M.R., Tormena, C.A., Karlen, D.L., 2017. Soil quality evaluation using the soil management assessment framework (SMAF) in Brazilian Oxisols with contrasting texture. Rev. Bras. Ci. Solo 41, e0160148.

Chhabra, A., Jensen, R.V., 1989. Direct determination of the f(α) singularity spectrum. Phys. Rev. Lett. 62 (12), 1327. https://doi.org/10.1103/PhysRevLett.62.1327

Chhabra, A.B., Meneveau, C., Jensen, R.V., Sreenivasan, K.R., 1989. Direct determination of the f(α) singularity spectrum and its application to fully developed turbulence. Phys. Rev. A. 40 (9), 5284–5294. https://doi.org/10.1103/PhysRevA.40.5284

Chun, H.C., Giménez, D., Yoon, S.W., 2008. Morphology, lacunarity and entropy of intra-aggregate pores: Aggregate size and soil management effects. Geoderma. 146 (1-2), 83-93. https://doi.org/10.1016/j.geoderma.2008.05.018

Chun, H.C., Gimenez, D., Yoon, S.W., Park, C.W., Moon, Y.H., Sonn, Y.K., Hyun, B.K., 2011. Review of Soil Structure Quantification from Soil Images. Korean J Soil Sci Fertil. 44 (3), 517-526. https://doi.org/10.7745/KJSSF.2011.44.3.517

Dal Ferro, N., Delmas, P., Duwig, C., Simonetti, G., Morari, F., 2012. Coupling X-ray microtomography and mercury intrusion porosimetry to quantify aggregate structures of a cambisol under different fertilisation treatments. Soil Tillage Res. 119, 13–21. https://doi.org/10.1016/j.still.2011.12.001

Dal Ferro, N., Sartori, L., Simonetti, G., Berti, A., Morari, F., 2014. Soil macro-and microstructure as affected by different tillage systems and their effects on maize root growth. Soil Tillage Res. 140, 55-65. https://doi.org/10.1016/j.still.2014.02.003

de Oliveira, J.A.T., Cássaro, F.A.M., Pires, L.F., 2021. Quantification of the pore size distribution of a Rhodic Hapludox under different management systems with X-ray microtomography and computational simulation. Soil Tillage Res. 209, 104941. https://doi.org/10.1016/j.still.2021.104941

Dong, P., 2000. Test of a new lacunarity estimation method for image texture analysis. Int. J. Remote Sens. 21 (17), 3369-3373. https://doi.org/10.1080/014311600750019985

Doube, M., Kłosowski, M.M., Arganda-Carreras, I., Cordelières, F.P., Dougherty, R.P., Jackson, J.S., Schmid, B., Hutchinson, J.R, Shefelbine, S.J., 2010. BoneJ: free and extensible bone image analysis in ImageJ. Bone. 47 (6), 1076-1079. https://doi.org/10.1016/j.bone.2010.08.023

Ferreira, T.R., Pires, L.F., Wildenschild, D., Brinatti, A.M., Borges, J.A., Auler, A.C., dos Reis, A. M., 2019. Lime application effects on soil aggregate properties: use of the mean weight diameter and synchrotron-based X-ray μCT techniques. Geoderma. 338, 585-596. https://doi.org/10.1016/j.geoderma.2018.10.035

Galdos, M.V., Pires, L.F., Cooper, H.V., Calonego, J.C., Rosolem, C.A., Mooney, S.J., 2019. Assessing the long-term effects of zero-tillage on the macroporosity of Brazilian soils using X-ray Computed Tomography. Geoderma. 337, 1126-1135. https://doi.org/10.1016/j.geoderma.2018.11.031

Galdos, M.V., Brown, E., Rosolem, C.A., Pires, L.F., Hallett, P.D., Mooney, S.J., 2020. Brachiaria species influence nitrate transport in soil by modifying soil structure with their root system. Sci. Rep. 10 (1), 1-11. https://doi.org/10.1038/s41598-020-61986-0

Gould, D.J., Vadakkan, T.J., Poché, R.A., Dickinson, M.E., 2011. Multifractal and lacunarity analysis of microvascular morphology and remodeling. Microcirculation. 18 (2), 136-151. https://doi.org/10.1111/j.1549-8719.2010.00075.x

Hammer, Ø., Harper, David A.T., Ryan, P.D., 2001. Paleontological statistics software package for education and data analysis. Paleontologia Electronica 4/1: 1–9.

Hillel, D., 2003. Introduction to environmental soil physics. Elsevier.

Imhoff, S., Ghiberto, P.J., Grioni, A., Gay, J.P., 2010. Porosity characterization of Argiudolls under different management systems in the Argentine Flat Pampa. Geoderma 158, 268–274.

Leiva, J.O., Silva, R.A., Buss, R.N., França, V.L., Souza, A.A., Siqueira, G.M., 2019. Multifractal analysis of soil penetration resistance under sugarcane cultivation. Rev. Bras. Eng. Agric. 23 (7), 538-544. https://doi.org/10.1590/1807-1929/agriambi.v23n7p538-544

Li, Zc., Hu, X., Li, Xy., 2019. Characterization of Root Architectures and Soil Macropore Networks Under Different Ecosystems Using X-ray CT Scanning in the Qinghai Lake Watershed, NE Qinghai–Tibet Plateau. J. Soil Sci. Plant Nutr. 19, 743-757.

Luo, L., Lin, H., 2009. Lacunarity and fractal analyses of soil macropores and preferential transport using micro-X-ray computed tomography. Vadose Zone Journal 8 (1), 233-241. https://doi.org/10.2136/vzj2008.0010

Mandelbrot, B.B. (1983). The fractal geometry of nature/Revised and enlarged edition. whf.

Martínez, F.S.J., Martín, M.A., Caniego, F.J., Tuller, M., Guber, A., Pachepsky, Y., García-Gutiérrez, C., 2010. Multifractal analysis of discretized X-ray CT images for the characterization of soil macropore structures. Geoderma. 156 (1-2), 32-42. https://doi.org/10.1016/j.geoderma.2010.01.004

Martínez, F.S.J., Caniego, F.J., García-Gutiérrez, C., 2017. Lacunarity of soil macropore space arrangement of CT images: effect of soil management and depth. Geoderma. 287, 80-89. https://doi.org/10.1016/j.geoderma.2016.09.007

Martinez-Carvajal, G.D., Oxarango, L., Adrien, J., Molle, P., Forquet, N., 2019. Assessment of X-ray Computed Tomography to characterize filtering media from Vertical Flow Treatment Wetlands at the pore scale. Science of the Total Environment. 658, 178-188. https://doi.org/10.1016/j.scitotenv.2018.12.119

Monreal, J.C., Martínez, F.S.J., Martí, J.I., Pérez-Gómez, R., 2013. Lacunarity of the spatial distributions of soil types in Europe. Vadose Zone Journal. 12(3), 1-9. https://doi.org/10.2136/vzj2012.0210

Munoz-Ortega, F.J., Martínez, F.S.J., Monreal, F.C., 2015. Volume, surface, connectivity and size distribution of soil pore space in CT images: comparison of samples at different depths from nearby natural and tillage areas. Pure Appl. Geophys. 172 (1), 167-179. https://doi.org/10.1007/s00024-014-0897-5

Pachepsky, Y.A., Giménez, D., Crawford, J.W., Rawls, W.J., 2000. Conventional and fractal geometry in soil science. In Developments in Soil Science. 27, 7-18. https://doi.org/10.1016/S0166-2481(00)80003-3

Pachepsky, Y.; Perfect, E.; Martin, M.A., 2006. Fractal geometry applied to soil and related hierarchical systems. Geoderma 134, 237-239. https://doi.org/10.1016/j.geoderma.2006.03.002

Panachuki, E., Bertol, I., Sobrinho, T.A., de Oliveira, P.T.S., Rodrigues, D.B.B., 2015. Effect of soil tillage and plant residue on surface roughness of na Oxisol under simulated rain. Rev. Bras. Ci. Solo 39, 268-278.

Peth, S., Horn, R., Beckmann, F., Donath, T., Fischer, J., Smucker, A.J.M., 2008. Three-dimensional quantification of intra-aggregate pore-space features using synchrotron-radiation-based microtomography. Soil Sci. Soc. Am. J. 72, 897-907.

Pires, L.F.; Bacchi, O.O.; Reichardt, K., 2004. Damage to soil physical properties caused by soil sampler devices as assessed by gamma ray computed tomography. Soil Res. 42 (7), 857-863. https://doi.org/10.1071/SR03167

Pires, L.F., Roque, W.L., Rosa, J.A., Mooney, S.J., 2019a. 3D analysis of the soil porous architecture under long term contrasting management systems by X-ray computed tomography. Soil Tillage Res. 191, 197-206. https://doi.org/10.1016/j.still.2019.02.018

Pires, L.F., Mooney, S.J., Auler, A.C., Atkinson, B., Sturrock, C. J., 2019b. X-ray microtomography to evaluate the efficacy of paraffin wax coating for soil bulk density evaluation. Geoderma. 337, 935-944. https://doi.org/10.1016/j.geoderma.2018.11.017

Posadas, A.N.D., Giménez, D., Quiroz, R., Protz, R., 2003. Multifractal Characterization of Soil Pore Systems. Soil Sci Soc Am J. 67 (5), 1361. https://doi.org/10.2136/sssaj2003.1361

Posadas, A.N.D., Quiroz, R., Zorogastua, P.E., León-Velarde, C., 2005. Multifractal characterization of the spatial distribution of ulexite in a Bolivian salt flat. Int. J. Remote Sens. 26 (3), 615-627. https://doi.org/10.1080/01431160512331299261

Posadas, A., Quiroz, R., Tannús, A., Crestana, S., Vaz, C. M., 2009. Characterizing water fingering phenomena in soils using magnetic resonance imaging and multifractal theory. Nonlinear Processes in Geophysics. 16 (1), 159.

Posadas, A.N.D., 2007. Characterizing and modeling preferential flow using magentic resonance imaging and multifractal theory. International Potato Center.

Roque, W.L., Souza, A.C.A. D., Barbieri, D.X., 2009. The Euler-Poincaré characteristic applied to identify low bone density from vertebral tomographic images. Rev Bras Reumatol. Campinas. 49 (2) (mar./abr. 2009), 140-152. https://doi.org/10.1590/S0482-50042009000200006

Roque, W.L., Arcaro, K., Lanfredi, R.B., 2012. Tortuosidade e conectividade da rede trabecular do rádio distal a partir de imagens microtomográficas. Rev. Bras. de Eng. Biomed. 28 (2), 116-123. http://dx.doi.org/10.4322/rbeb.2012.017

Roy, A., Perfect, E., 2014. Lacunarity analyses of multifractal and natural grayscale patterns. Fractals. 22 (03), 1440003. https://doi.org/10.1142/S0218348X14400039

Roy, A., Perfect, E., Dunne, W.M., McKay, L.D., 2014. A technique for revealing scale-dependent patterns in fracture spacing data. J. Geophys. Res. Solid Earth. 119 (7), 5979-5986. https://doi.org/10.1002/2013JB010647

Sá, J.C.M., Séguy, L., Tivet, F., Lal, R., Bouzinac, S., Borszowskei, P.R., Briedis, C., dos Santos, J.B., Hartman, D.C., Bertoloni, C.G., Rosa, J., Friedrich, T., 2015. Carbon depletion by plowing and its restoration by no-till cropping systems in Oxisols of Subtropical and Tropical agro-ecoregions in Brazil. Land Degrad. Develop. 26, 531-543.

Santos, C.R.D., Antonino, A.C.D., Heck, R.J., Lucena, L.R.R.D., Oliveira, A.C.H.D., Silva, A. S. A. D., Stosic, B., Menezes, R. S. C., 2020. 3D soil void space lacunarity as an index of degradation after land use change. Acta Sci. Agron. 42. https://doi.org/10.4025/actasciagron.v42i1.42491

Sampurno, J., Azwar, A., Latief, F.D.E., Srigutomo, W., 2016. Multifractal characterization of pore size distributions of peat soil. J. Math. Fundam. Sci. 48 (2), 106-114. https://doi.org/10.5614/j.math.fund.sci.2015.48.2.2

Sarkar, N., Chaudhuri, B.B., 1995. Multifractal and generalized dimensions of gray-tone digital images. Signal Process. 42 (2), 181-190. https://doi.org/10.1016/0165-1684(94)00126-K

Siqueira, G.M., Silva, Ê.D.F., Montenegro, A.D., Vidal Vázquez, E., Paz-Ferreiro, J., 2013. Multifractal analysis of vertical profiles of soil penetration resistance at the field scale. Nonlinear Process Geophys. 20 (4). https://doi.org/10.5194/npg-20-529-2013

Soil Survey Staff, 2013. Simplified Guide to Soil Taxonomy. USDA-Natural Resources Conservation Service, National Soil Survey Center, Lincoln, USA

Soto-Gómez, D., Perez-Rodriguez, P., Juiz, L.V., Paradelo, M., Lopez-Periago, J.E., 2020. 3D multifractal characterization of computed tomography images of soils under different tillage management: Linking multifractal parameters to physical properties. Geoderma, 363, 114129. https://doi.org/10.1016/j.geoderma.2019.114129

Szczepaniak, A., Macek, W.M., 2008. Asymmetric multifractal model for solar wind intermittent turbulence. Nonlinear Process Geophys. 15 (4), 615-620. https://doi.org/10.5194/npg-15-615-2008

Tavares Filho, J., Tessier, D., 2009. Characterization of soil structure and porosity under long-term conventional tillage and no-tillage systems. Rev. Bras. Ciênc. Solo. 33 (6), 1837-1844. https://doi.org/10.1590/S0100-06832009000600032

Torre, I.G., Losada, J.C., Heck, R.J., Tarquis, A.M., 2018. Multifractal analysis of 3D images of tillage soil. Geoderma. 311, 167-174. https://doi.org/10.1016/j.geoderma.2017.02.013

Tseng, C.L., Alves, M.C. Crestana, S., 2018. Quantifying physical and structural soil properties using X-ray microtomography. Geoderma. 318, 78-87. https://doi.org/10.1016/j.geoderma.2017.11.042

Wang, D., Fu, B., Zhao, W., Hu, H., Wang, Y., 2008. Multifractal characteristics of soil particle size distribution under different land-use types on the Loess Plateau, China. Catena. 72 (1), 29-36. https://doi.org/10.1016/j.catena.2007.03.019

Wang, J., Qin, Q., Guo, L., Feng, Y., 2018. Multi-fractal characteristics of three-dimensional distribution of reconstructed soil pores at opencast coal-mine dump based on high-precision CT scanning. Soil Tillage Res. 182, 144-152. https://doi.org/10.1016/j.still.2018.05.013

Wang, J., Guo, L., Bai, Z., 2017. Variations in pore distribution of reconstructed soils induced by opencast mining and land rehabilitation based on computed tomography images. Archives of Agronomy and Soil Science 63, 1685-1696. https://doi.org/10.1080/03650340.2017.1304638

Zhu, F., Liao, J., Xue, S., Hartley, W., Zou, Q., Wu, H., 2016. Evaluation of aggregate microstructures following natural regeneration in bauxite residue as characterized by synchrotron-based X-ray micro-computed tomography. Science of the Total Environment. 573, 155-163. https://doi.org/10.1016/j.scitotenv.2016.08.108

Table captions

Table 1

Multifractal parameters calculated from 3D multifractal spectrum curves for the area under secondary forest (F) and for the three soil management systems (conventional tillage - CT, minimum tillage - MT and no-tillage - NT).

Management systems	F	CT	MT	NT
Δ	1.44±0.07	1.44±0.06	1.36±0.09	1.45±0.04
A	0.57±0.08[a]	0.34±0.04[b]	0.40±0.04[b]	0.66±0.07[c]
$\alpha_{máx}$	4.05±0.06[a]	4.19±0.07[b]	4.09±0.07[ab]	3.99±0.04[a]
$f(\alpha_{máx})$	2.85±0.02[a]	2.92±0.03[b]	2.90±0.01[b]	2.83±0.02[a]

Results under same parameter followed by the same letter indicate that there are no statistical differences between the data analyzed (Tukey test $p<0,05$). Δ - Degree of multifractality. A – Degree of asymmetry. α_{max} – Related to internal system energy. $f(\alpha_{max})$ - Related to the global entropy of the system (Boltzmann entropy).

Table 2

3D geometric parameters of the porous system for the area under secondary forest (F) and for the three soil management systems (conventional tillage - CT, minimum tillage - MT and no-tillage – NT).

Management systems	F	CT	MT	NT
DA	0.16±0.07	0.14±0.02	0.19±0.07	0.15±0.04
C	3.26±0.56[a]	10.17±5.15[b]	5.61±2.48[ab]	2.64±0.58[a]
τ	1.41±0.05[a]	1.30±0.04[b]	1.31±0.03[b]	1.52±0.07[c]

Results under same parameter followed by the same letter indicate that there are no statistical differences between the data analyzed (Tukey's test $p<0,05$). DA - Degree of anisotropy. C - Pore connectivity. τ – Pore Tortuosity.

Figures

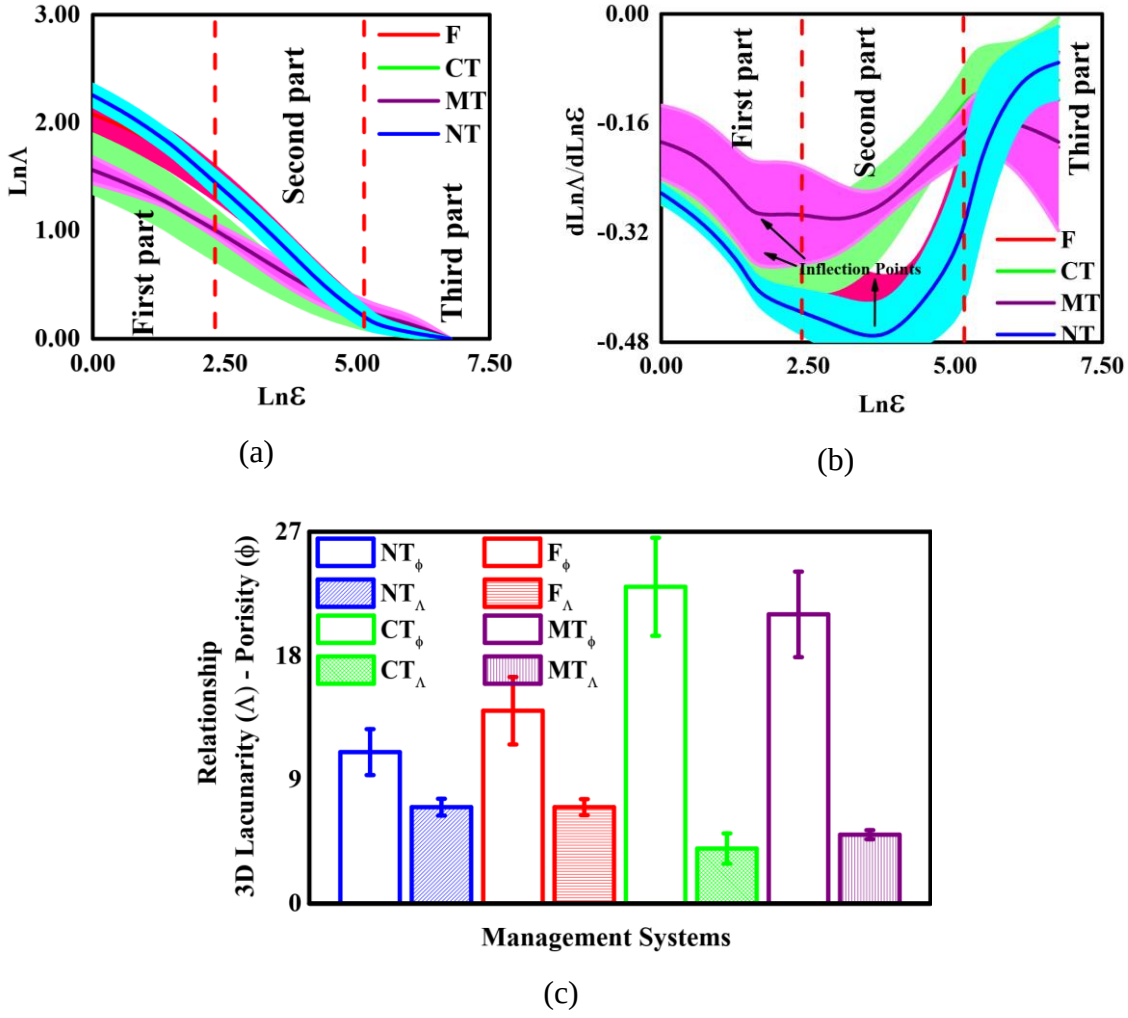

Fig. 1. (a) 3D lacunarities and (b) its first derivative for the area under secondary forest (F) and for the three soil management systems (conventional tillage- CT, minimum tillage - MT and no-tillage - NT). The lighter colors around the solid lines indicate the standard deviation from the mean. (c) Relationship between 3D lacunarity and porosity. Divisions into three parts are due to the best linear adjustments for each part and evidence of this linear behavior, and in the case of derivatives, for better visualization of the inflection points.

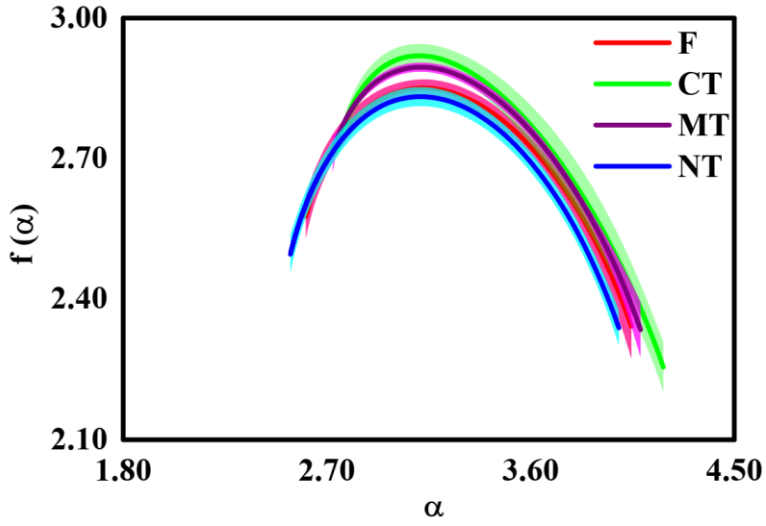

Fig. 2. 3D multifractal spectra for area under secondary forest (F) and the three soil tillage systems (conventional tillage – CT, minimum tillage – MT and no- tillage – NT). The lighter colors around the solid lines indicate the standard deviation from the mean.

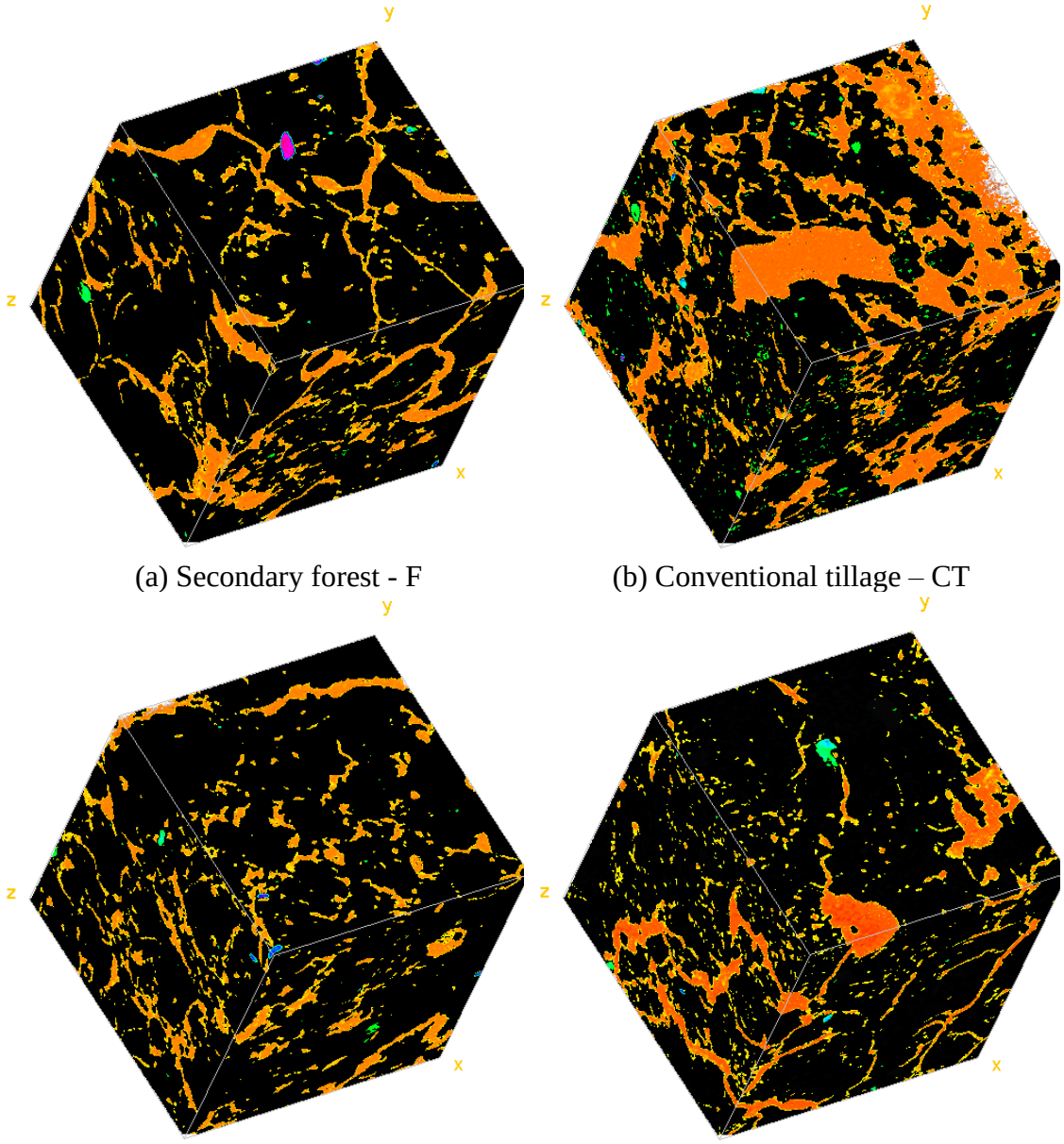

(a) Secondary forest - F (b) Conventional tillage – CT

(c) Minimum tillage – MT (d) No-tillage – NT

Fig. 3. 3D views the pore distribution inside the soil samples submitted to contrasting management practices (CT, MT and NT) and the area under secondary forest (F). In orange (large connected pores)/yellow (small or isolated pores) is represented the pores, in green materials with intermediate densities, and in blue/violet materials with high densities (small particles), and in black is the soil matrix.

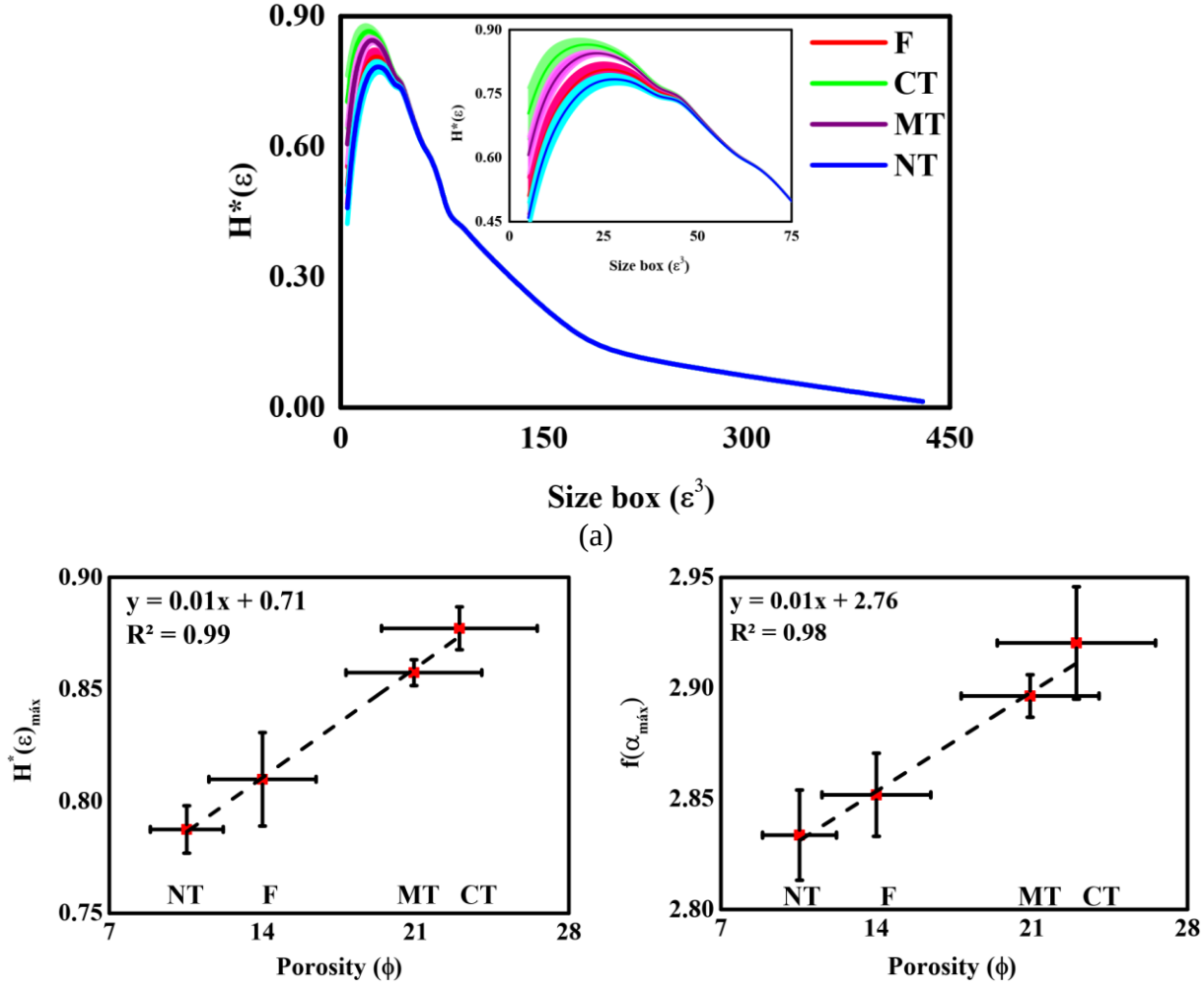

Fig. 4. (a) Normalized 3D Shannon entropy for the area under secondary forest (F) and the three different soil tillage systems (conventional tillage - CT, minimum tillage - MT, and no-tillage - NT). The lighter colors around the solid lines indicate the standard deviation from the mean. (b) Relationship between maximum normalized 3D Shannon entropy and porosity. (c) Relationship between global or Boltzmann's entropy and porosity.